

Chapter 10

Phenomenology of the Weak Interaction

The discovery and the first theories of the weak interaction were based on the phenomenology of β -decay. Bound states formed by the weak interaction are not known, in contrast to those of the electromagnetic, strong and gravitational interactions. The weak interaction is in this sense somewhat foreign. We cannot, for example, base its description on any analogous phenomena in atomic physics. The weak interaction is, however, responsible for the decay of quarks and leptons.

In scattering experiments weak interaction effects are difficult to observe. Reactions of particles which are solely subject to the weak interaction (neutrinos) have extremely tiny cross-sections. In scattering experiments involving charged leptons and hadrons the effects of the weak interaction are clouded by those of the strong and electromagnetic interactions. Thus, most of our knowledge of the weak interaction has been obtained from particle decays.

The first theoretical description of β -decay, due to Fermi [12], was constructed analogously to that of the electromagnetic interaction. With some modifications, it is still applicable to low-energy processes. Further milestones in the investigation of the weak interaction were the discovery of parity violation [21], of different neutrino families [11] and of CP violation in the K^0 system [8].

Quarks and leptons are equally affected by the weak interaction. In the previous chapter we discussed the quarks at length. We now want to treat the leptons in more detail before we turn to face the phenomena of the weak interaction.

10.1 Properties of Leptons

Charged leptons In our treatment of e^+e^- scattering we encountered the charged leptons: the electron (e), the muon (μ) and the tau (τ) as well as their antiparticles (the e^+ , μ^+ and τ^+) which have the same masses as their partners but are oppositely charged.

The electron and the muon are the lightest electrically charged particles. Charge conservation thus ensures that the electron is stable and that an electron is produced when a muon decays. Muon decay proceeds via

$$\mu^- \rightarrow e^- + \bar{\nu}_e + \nu_\mu.$$

In a very few cases an additional photon or e^+e^- pair is produced. The energetically allowed process

$$\mu^- \not\rightarrow e^- + \gamma,$$

is, on the other hand, never observed. The muon is therefore not just an excited state of the electron.

The τ -lepton is much heavier than the muon and, indeed, more so than many hadrons. Thus it does not have to decay solely into lighter leptons

$$\tau^- \rightarrow e^- + \bar{\nu}_e + \nu_\tau \quad \tau^- \rightarrow \mu^- + \bar{\nu}_\mu + \nu_\tau,$$

but can also turn into hadrons, e.g., into a pion and a neutrino

$$\tau^- \rightarrow \pi^- + \nu_\tau.$$

In fact more than half of all τ decays follow the hadronic route [4].

Neutrinos We have already seen several processes in which neutrinos are produced: nuclear β -decay and the decays of charged leptons. Neutrinos are electrically neutral leptons and, as such, do not feel the electromagnetic or strong forces. Since neutrinos interact only weakly, they can as a rule only be detected indirectly in processes where charged particles are produced. Typically the energy, momentum and spin carried away or brought in by the neutrino is determined by measuring the other particles involved in the reaction and applying conservation laws. For example, the sums of the energies and angular momenta of the observed particles in β -decays indicate that another particle as well as the electron must also have been emitted. Experiment has made it completely clear that neutrinos and antineutrinos are distinct particles. The antineutrinos produced in a β -decay

$$n \rightarrow p + e^- + \bar{\nu}_e$$

for example, only induce further reactions in which positrons are produced and do not lead to electrons being created:

$$\begin{aligned} \bar{\nu}_e + p &\rightarrow n + e^+ \\ \bar{\nu}_e + n &\not\rightarrow p + e^- . \end{aligned}$$

Neutrinos and antineutrinos produced in charged pion decays

$$\begin{aligned}\pi^- &\rightarrow \mu^- + \bar{\nu}_\mu \\ \pi^+ &\rightarrow \mu^+ + \nu_\mu\end{aligned}$$

also behave differently. They are distinct particles: neutrinos from π^+ decays only generate negatively charged muons, while antineutrinos from π^- decays only produce positive muons. Furthermore, they induce reactions in which μ^- or μ^+ are created but never produce electrons or positrons [11]. This implies that the electron neutrino ν_e and the muon neutrino ν_μ are different sorts of neutrinos: an electron neutrino, which is associated with the creation and annihilation of electrons, and a muon neutrino, which we similarly associate with the muon. Accordingly we can assign a tau neutrino ν_τ to the tau lepton.

Thus, we may conclude that there are three sorts of neutrinos: the electron neutrino ν_e associated with the creation or annihilation of electrons, the muon neutrino ν_μ allocated to the muon, and the tau neutrino ν_τ , assigned to the tau lepton.

The lepton families We now know a total of six different leptons. Three of them (e^- , μ^- , τ^-) are electrically charged, the other three, the neutrinos (ν_e , ν_μ , ν_τ), are neutral. To each of them there exists an antiparticle. We denote the various types of leptons as *leptonic flavour* in analogy to the classification of the six types of quarks by their flavour u, d, c, s, t and b (cf. Sect. 7.4). All leptons have spin- $\frac{1}{2}$ and are therefore fermions. We have seen that the three charged leptons and their neutrinos are intimately connected and, therefore, denote them in three families, each of which is made up of two particles whose charges differ by one unit:

$$\begin{pmatrix} \nu_e \\ e^- \end{pmatrix} \quad \begin{pmatrix} \nu_\mu \\ \mu^- \end{pmatrix} \quad \begin{pmatrix} \nu_\tau \\ \tau^- \end{pmatrix}.$$

The neutrinos in the upper row are electrically neutral, the leptons in the lower row have charge $-1e$. The charged leptons have, like the quarks, very different masses: ($m_\mu/m_e \approx 207$, $m_\tau/m_\mu \approx 17$). To each of these families there exists the corresponding family of antiparticles.

There is one important difference between neutrinos and charged leptons in addition to their charge: the otherwise very successful standard model of particle physics (cf. Chap. 13) predicts neutrinos to be massless. From neutrino oscillations, that we will discuss in the subsequent chapter, we learn, however, that neutrinos must possess a mass. As a consequence, a neutrino from one family, e.g., an electron neutrino ν_e , can transmute into a neutrino of another family, e.g., a tau neutrino ν_τ . The masses of the neutrinos are still unknown, we only know the differences of their masses squared. Details will be discussed in Sects. 11.2 and 11.3.

Despite intensive searches at ever higher energies, no further leptons have yet been found. The lower bound for the mass of any further charged lepton is currently approximately $100 \text{ GeV}/c^2$ and of any further neutral lepton approximately $40 \text{ GeV}/c^2$. In Sect. 12.2 we will see that there cannot be more than three light

neutrinos ($m_\nu \ll 10 \text{ GeV}/c^2$). We still do not have a generally accepted reason for why the fundamental fermions come in three families and we do not understand their masses.

Lepton number conservation In all the reactions we have mentioned above, the creation or annihilation of a lepton was always associated with the creation or annihilation of an antilepton of the same flavour family. To our present knowledge this is true for all reactions. As with the baryons, we therefore have a conservation law: in all reactions the number of leptons of a particular family minus the number of the corresponding antileptons is conserved. We write

$$L_\ell = N(\ell) - N(\bar{\ell}) + N(\nu_\ell) - N(\bar{\nu}_\ell) = \text{const.}, \quad \text{where } \ell = e, \mu, \tau. \quad (10.1)$$

The L_ℓ 's are individually referred to as *lepton family numbers* and the sum $L = L_e + L_\mu + L_\tau$ is called *lepton number*.

In consequence the following production reactions are allowed or forbidden:

	Allowed		Forbidden
$p + \mu^-$	$\rightarrow \nu_\mu + n$		$p + \mu^- \not\rightarrow \pi^0 + n$
$e^+ + e^-$	$\rightarrow \nu_\mu + \bar{\nu}_\mu$		$e^+ + e^- \not\rightarrow \nu_e + \nu_\mu$
π^-	$\rightarrow \mu^- + \bar{\nu}_\mu$		$\pi^- \not\rightarrow e^- + \nu_e$
μ^-	$\rightarrow e^- + \bar{\nu}_e + \nu_\mu$		$\mu^- \not\rightarrow e^- + \bar{\nu}_\mu + \nu_e$
τ^-	$\rightarrow \pi^- + \nu_\tau$		$\tau^- \not\rightarrow \pi^- + \nu_e$

Experimentally the upper limits for any violation of the lepton family number L_ℓ or the lepton number L in electromagnetic and weak decays are very small. Examples are [19]

$$\frac{\Gamma(\mu^\pm \rightarrow e^\pm \gamma)}{\Gamma(\mu^\pm \rightarrow \text{all channels})} < 2.4 \cdot 10^{-12} \quad (L_\ell)$$

$$\frac{\Gamma(\tau^- \rightarrow e^+ \pi^- \pi^-)}{\Gamma(\tau^- \rightarrow \text{all channels})} < 8.8 \cdot 10^{-8} \quad (L). \quad (10.2)$$

Note though that this conservation rule only really refers to production processes. Neutrino oscillations lead to a change of lepton family numbers and so only lepton number as a whole is truly conserved. Many theorists believe that neutrinos are so-called Majorana-particles. This would lead to a small violation of the lepton number, cf. Sect. 11.4. The only realistic hope for the observation of this effect is the neutrinoless double β -decay, which we will treat in some detail in Sect. 18.7.

All the allowed reactions that we have listed above proceed exclusively through the weak interaction, since in all these cases neutrinos are involved and these particles are only subject to the weak interaction. The opposite conclusion is,

however, incorrect. We will see in the following section that there are indeed weak processes which involve neither neutrinos nor any other leptons.

10.2 The Types of Weak Interactions

Recall that the weak interaction can transform a charged lepton into its family's neutrino and that it can produce a charged lepton (antilepton) and its antineutrino (neutrino). In just the same manner quarks of one flavour can be transformed into quarks with another flavour in weak interactions: a typical example of this is the transformation of a d-quark into a u-quark – this takes place in the β -decay of a neutron. In all such reactions the identity of the quarks and leptons involved changes and, simultaneously, the charge changes by $+1e$ or $-1e$. The term *charged current* was coined to describe such reactions. They are mediated by charged particles, the W^+ and W^- .

For a long time only this type of weak interaction was known. Nowadays we know that weak interactions may also proceed via the exchange of an additional, electrically neutral particle, the Z^0 . In these reactions the quarks and leptons are not changed. One refers to them as *neutral currents*.

The W^\pm and the Z^0 are vector bosons, i.e., they have spin-1. Their masses are large: $80 \text{ GeV}/c^2$ (W^\pm) and $91 \text{ GeV}/c^2$ (Z^0). We will return to their experimental detection in Sect. 12.1. In this chapter we will, following the historical development, initially concern ourselves with the *charged currents*. These may be straightforwardly divided up into three categories (Fig. 10.1): *leptonic processes*, *semileptonic processes* and *non-leptonic processes*.

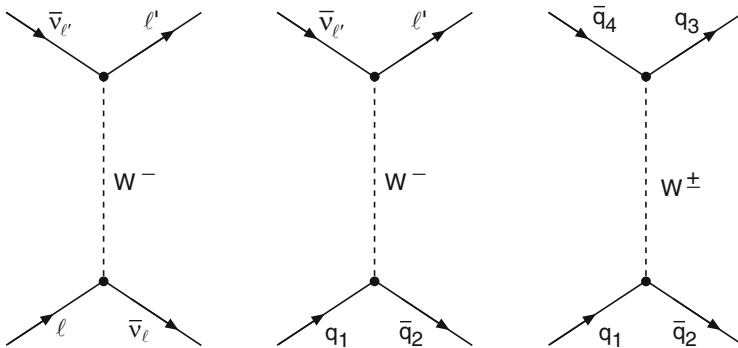
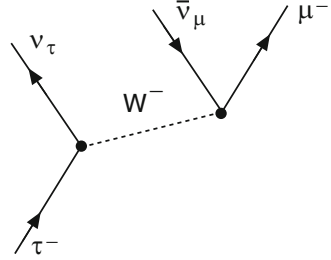


Fig. 10.1 The three sorts of charged current reactions: a leptonic process (*left*), a semileptonic process (*middle*) and a non-leptonic process (*right*)

Fig. 10.2 Leptonic decay of the τ -lepton



Leptonic processes If the W boson only couples to leptons, one speaks of a leptonic process. The underlying reaction is

$$\ell + \bar{\nu}_\ell \longleftrightarrow \ell' + \bar{\nu}_{\ell'}$$

Examples of this reaction are the leptonic decay of the τ -lepton (Fig. 10.2):

$$\tau^- \rightarrow \mu^- + \bar{\nu}_\mu + \nu_\tau$$

$$\tau^- \rightarrow e^- + \bar{\nu}_e + \nu_\tau$$

and the scattering process

$$\nu_\mu + e^- \rightarrow \mu^- + \nu_e$$

Semileptonic processes *Semileptonic processes* are those where the exchanged W boson couples to both leptons and quarks. The fundamental process here is

$$q_1 + \bar{q}_2 \longleftrightarrow \ell + \bar{\nu}_\ell$$

A prominent example is the β -decay of a neutron (Fig. 10.3) which may be reduced to the decay of a d -quark in which the two other quarks are not involved. The latter are called *spectator quarks*. Inverse reactions are processes such as the inverse β -decay $\bar{\nu}_e + p \rightarrow n + e^+$ or $\nu_e + n \rightarrow p + e^-$ and electron capture $p + e^- \rightarrow n + \nu_e$. (Anti-)Neutrinos were directly detected for the first time in the first of these reactions [10] – antineutrinos from the β^- -decay of neutron-rich fission products were seen to react with hydrogen. The second reaction may be used to detect solar and stellar neutrinos emanating from β^+ -decays of proton-rich nuclei produced in fusion reactions.

Further examples of semileptonic processes are charged pion or kaon decay:

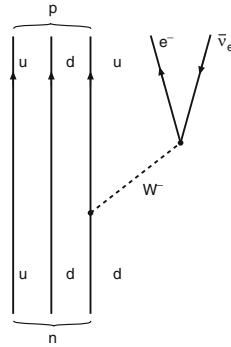


Fig. 10.3 Semileptonic decay of the neutron

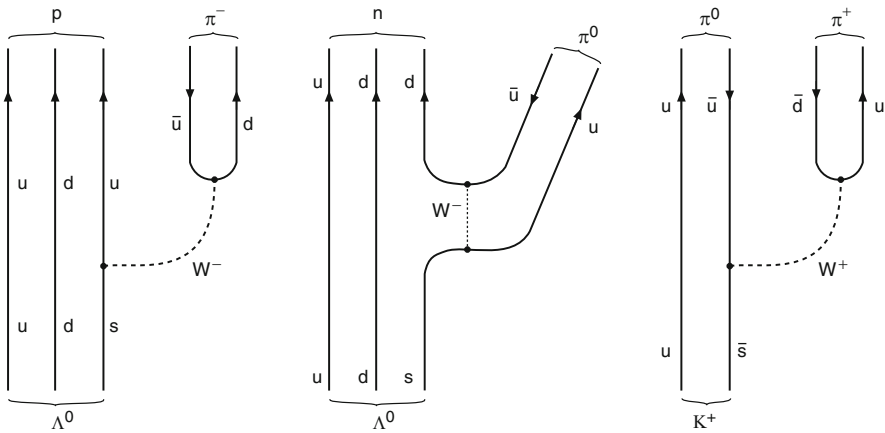


Fig. 10.4 Non-leptonic decays of the Λ^0 hyperon (*left, middle*) and of the K^+ meson (*right*)

Hadron description	Quark description
$\pi^- \rightarrow \mu^- + \bar{\nu}_\mu$	$d + \bar{u} \rightarrow \mu^- + \bar{\nu}_\mu$
$K^- \rightarrow \mu^- + \bar{\nu}_\mu$	$s + \bar{u} \rightarrow \mu^- + \bar{\nu}_\mu$,

or deep-inelastic neutrino-nucleon scattering, which we will treat in more detail in Sect. 10.6.

Non-leptonic processes Finally non-leptonic processes do not involve leptons at all. The basic reaction is

$$q_1 + \bar{q}_2 \longleftrightarrow q_3 + \bar{q}_4.$$

Charge conservation requires that the only allowed quark combinations have a total charge $\pm 1e$. Examples are the hadronic decays of baryons and mesons with strangeness, such as the decay of the Λ^0 hyperon into a nucleon and a pion, or that of K^+ ($u\bar{s}$) into two pions (Fig. 10.4).

10.3 Coupling Strength of the Weak Interaction

We now want to deal with charged currents in a more quantitative manner. We will treat leptonic processes in what follows since leptons, in contrast to quarks, exist as free particles which simplifies matters.

As with Mott scattering or e^+e^- annihilation, the transition matrix element for such processes is proportional to the square of the *weak charge* g to which the W Boson couples and to the propagator (4.23) of a massive spin-1 particle:

$$\mathcal{M}_{fi} \propto g \cdot \frac{1}{Q^2 c^2 + M_W^2 c^4} \cdot g \xrightarrow{Q^2 \rightarrow 0} \frac{g^2}{M_W^2 c^4}. \quad (10.3)$$

The difference to an electromagnetic interaction is seen in the finite mass of the exchange particle. Instead of the photon propagator $(Qc)^{-2}$, we see a propagator which is almost a constant for small enough momenta $Q^2 \ll M_W^2 c^2$. We will see in Sect. 12.2 that the weak charge g and the electric charge e are of a similar size. In fact, g is slightly larger than e . The very large mass of the exchange boson means that at small Q^2 the weak interaction appears to be much weaker than the electromagnetic interaction. It also means that its range $\hbar/M_W c \approx 2.5 \cdot 10^{-3}$ fm is very limited.

In the approximation of small four-momentum transfers one may then describe this interaction as a point-like interaction of the four particles involved (Fig. 10.5). This was in fact the original description of the weak interaction before the idea of the W and Z bosons was brought in. The coupling strength of this interaction is described by the *Fermi constant* G_F , which is proportional to the square of the weak charge g , very much as the electromagnetic coupling constant $\alpha = e^2/(4\pi\epsilon_0\hbar c)$ is

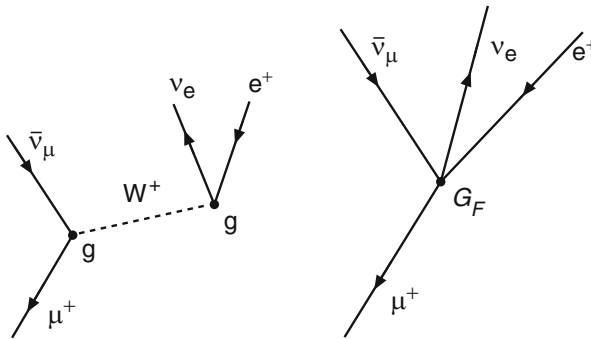


Fig. 10.5 Sketch of the leptonic muon decay with the exchange of a W^+ boson (*left*) and as point-like interaction (*right*)

proportional to the square of the electric charge e . It is so defined that $G_F/(\hbar c)^3$ has dimensions of $[1/\text{energy}^2]$ and is related to g by

$$\frac{G_F}{\sqrt{2}} = \frac{\pi\alpha}{2} \cdot \frac{g^2}{e^2} \cdot \frac{(\hbar c)^3}{M_W^2 c^4}. \quad (10.4)$$

The decay of the muon The most exact value for the Fermi constant is obtained from muon decay. The muon decays, as explained in Sect. 10.1, by

$$\mu^- \rightarrow e^- + \bar{\nu}_e + \nu_\mu, \quad \mu^+ \rightarrow e^+ + \nu_e + \bar{\nu}_\mu.$$

Since the muon mass is tiny compared to that of the W boson, it is reasonable to treat this interaction as point-like and to describe the coupling via the Fermi constant.

In this approximation the lifetime of the muon may be calculated with the help of the golden rule, if we use the Dirac equation and take into account the amount of phase space available to the three outgoing leptons. One finds that the decay width is:

$$\Gamma_\mu = \frac{\hbar}{\tau_\mu} = \frac{G_F^2}{192\pi^3(\hbar c)^6} \cdot (m_\mu c^2)^5 \cdot (1 + \varepsilon). \quad (10.5)$$

The correction term ε , which reflects higher order (radiative) corrections and phase-space effects resulting from the finite electron mass, is small (see Eq. 5 in [16]). It should be noted that the transition rate is proportional to the fifth power of the energy and hence the mass of the decaying muon. In Sect. 16.6 we will show in detail how the phase space may be calculated and how the E^5 -dependence can be derived (in the example of the β -decay of the neutron).

The muon mass and lifetime have been measured to a high precision:

$$\begin{aligned} m_\mu &= (105.6583715 \pm 0.0000035) \text{ MeV}/c^2, \\ \tau_\mu &= (2.1969811 \pm 0.0000022) \cdot 10^{-6} \text{ s}. \end{aligned} \quad (10.6)$$

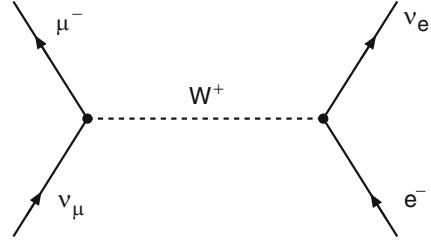
This yields a value for the Fermi constant

$$\frac{G_F}{(\hbar c)^3} = (1.1663787 \pm 0.0000006) \cdot 10^{-5} \text{ GeV}^{-2} \approx \frac{1.03 \cdot 10^{-5}}{(M_p c^2)^2}. \quad (10.7)$$

Neutrino-electron scattering Neutrino-electron scattering is a reaction between free, elementary particles. It proceeds exclusively through the weak interaction. We can discuss the effects of the effective coupling strength G_F on the cross-section of this reaction and show why the weak interaction is called “weak”.

In Fig. 10.6 the scattering of muon neutrinos off electrons in which the ν_μ is changed into a μ^- is shown.

Fig. 10.6 Sketch of the charged-current reaction $\nu_\mu e^- \rightarrow \mu^- \nu_e$



We have chosen this process as our example since it can only take place via W -exchange.

For small four-momenta the total cross-section for neutrino-electron scattering is proportional to the square of the effective coupling constant G_F . Similarly to our discussion of the total cross-section in e^+e^- annihilation in Sect. 9.1, the characteristic length and energy scales of the reaction (the constants $\hbar c$ and the centre-of-mass energy \sqrt{s}) must enter the cross-section in such a way as to yield the correct dimensions (area):

$$\sigma = \frac{G_F^2}{\pi(\hbar c)^4} \cdot s, \quad (10.8)$$

where s may be found in the laboratory frame from (9.3) to be $s = 2m_e c^2 E_\nu$. From (10.7) one finds that the cross-section in the laboratory frame is

$$\sigma_{\text{lab}} = 1.7 \cdot 10^{-41} \text{ cm}^2 \cdot E_\nu / \text{GeV}. \quad (10.9)$$

This is an extremely tiny cross-section. To illustrate this point we now estimate the distance L which a neutrino must traverse in iron until it may weakly interact with an electron. The electron density in iron is

$$n_e = \frac{Z}{A} \rho N_A \approx 22 \cdot 10^{23} \text{ cm}^{-3}. \quad (10.10)$$

For neutrinos with an energy of 1 MeV the mean free path is therefore $L = (n_e \cdot \sigma)^{-1} = 2.6 \cdot 10^{17} \text{ m}$, which is about 30 light years!¹

At very high energies the simple formula (10.9) is no longer valid, since the cross-section would limitlessly grow with the neutrino energy. This of course will not happen in practice: at large four-momentum transfers $Q^2 \gg M_W^2 c^2$ the propagator term primarily determines the energy dependence of the cross-section. The approximation of a point-like interaction no longer holds. At a fixed centre-of-mass

¹The absorption of neutrinos by the atomic nuclei is neglected here. This is a reasonable approximation for neutrino energies less than 1 MeV, but would need to be modified for higher energies.

energy \sqrt{s} the cross-section falls off, as in electromagnetic scattering, as $1/Q^4$. The total cross-section is on the other hand [9]:

$$\sigma = \frac{G_F^2}{\pi(\hbar c)^4} \cdot \frac{M_W^2 c^4}{s + M_W^2 c^4} \cdot s. \quad (10.11)$$

It does not increase linearly with s , as the point-like approximation implies, rather it asymptotically approaches a constant value.

Neutral currents Up to now we have only considered neutrino-electron scattering via W^+ exchange, i.e., through charged currents. Neutrinos and electrons can, however, interact via Z^0 exchange, i.e., neutral-current interactions are possible. The Z^0 changes neither the mass nor the charge of the involved particles.

Elastic muon-neutrino scattering off electrons, $\nu_\mu e^- \rightarrow \nu_\mu e^-$ (Fig. 10.7), is particularly suitable for investigating the weak interaction via Z^0 exchange. This is because conservation of lepton family number precludes W exchange. Reactions of this kind were first seen in 1973 at CERN [14]. This was the first experimental signal for weak neutral currents.

We can estimate the total cross-section for the reaction $\nu_\mu e^- \rightarrow \nu_\mu e^-$ for small four-momenta by repeating the calculation we did for the scattering via charged currents but modifying the coupling G_F . The only difference between the two interactions is in the mass of the two exchange bosons. The mass of the exchange boson squared appears in the propagator, so that the G_F should be multiplied by $M_W^2/M_{Z^0}^2 \approx 0.78$. The total cross-section at low energies reads then

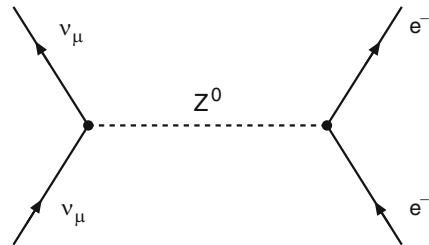
$$\sigma = \frac{M_W^4}{M_{Z^0}^4} \cdot \frac{G_F^2}{\pi(\hbar c)^4} \cdot s, \quad (10.12)$$

or

$$\sigma(\nu_\mu e^- \rightarrow \nu_\mu e^-) \approx 0.6 \cdot \sigma(\nu_\mu e \rightarrow \mu^- \nu_e). \quad (10.13)$$

Calculating $\nu_e e^-$ scattering is more complicated since both Z and W exchange lead to the same final state and thus interfere with each other.

Fig. 10.7 Sketch of the neutral-current reaction $\nu_\mu e^- \rightarrow \nu_\mu e^-$



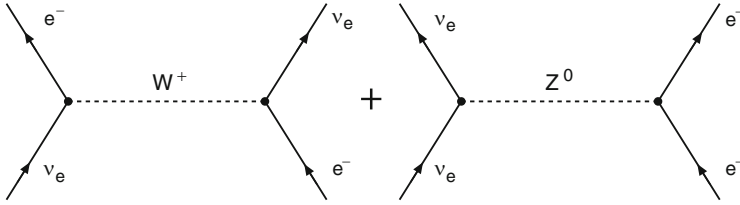


Fig. 10.8 Superposition of the charged-current reaction (*left*) and the neutral-current reaction (*right*) in the process $\nu_e e^- \rightarrow \nu_e e^-$

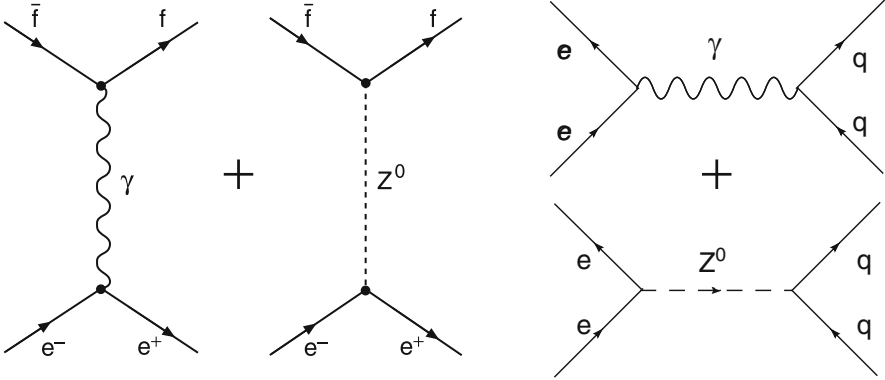


Fig. 10.9 Superposition of the electromagnetic and weak interaction in $e^+ e^-$ annihilation (*left*) and for electron-quark scattering (*right*)

Normally weak interactions via neutral currents will be hardly observed, since they will be superposed by the much stronger electromagnetic interaction and in case of the quarks by the strong interaction. In electron-positron annihilation (Fig. 10.9(left)) or for electron-quark scattering (Fig. 10.9(right)) a superposition of the weak and the electromagnetic interactions occurs.

Only when the centre-of-mass energy is comparable to the mass of the Z^0 the two interactions become comparably large (cf. Sect. 12.2). The interference between the weak and the electromagnetic neutral currents has been observed very clearly in experiments at the electron-positron collider LEP and in deep-inelastic scattering at very high Q^2 at HERA (cf. Sect. 12.2).

Universality of the weak interaction If we assume that the weak charge g is the same for all quarks and leptons, then (10.5) must hold for all possible charged decays of the fundamental fermions into lighter leptons or quarks. All the decay channels then contribute equally to the total decay width, up to a phase-space correction coming from the different masses.

We choose to consider the example of the decay of the τ -lepton. This particle has essentially three routes open to it

$$\begin{aligned}\tau^- &\rightarrow \nu_\tau + \bar{\nu}_e + e^- \\ \tau^- &\rightarrow \nu_\tau + \bar{\nu}_\mu + \mu^- \\ \tau^- &\rightarrow \nu_\tau + \bar{u} + d,\end{aligned}\tag{10.14}$$

whose widths are $\Gamma_{\tau e} \approx \Gamma_{\tau\mu}$ and $\Gamma_{\tau d\bar{u}} \approx 3\Gamma_{\tau\mu}$.² The factor of three follows from the $\bar{u}d$ -pair having the possibility of appearing in three different colour combinations ($\bar{r}r$, $\bar{b}b$, $\bar{g}g$).

From the mass term in (10.5) we have:

$$\Gamma_{\tau e} = (m_\tau/m_\mu)^5 \cdot \Gamma_{\mu e},\tag{10.15}$$

and the lifetime is thus predicted to be:

$$\tau_\tau = \frac{\hbar}{\Gamma_{\tau e} + \Gamma_{\tau\mu} + \Gamma_{\tau d\bar{u}}} \approx \frac{\tau_\mu}{5 \cdot (m_\tau/m_\mu)^5} \approx 3.1 \cdot 10^{-13} \text{ s}.\tag{10.16}$$

Experimentally we find [19]

$$\tau_\tau^{\text{exp}} = (2.906 \pm 0.010) \cdot 10^{-13} \text{ s}.\tag{10.17}$$

This good agreement confirms that quarks occur in three different colours and is strongly supportive of the quark and lepton weak charges being identical.

10.4 The Quark Families

We have claimed that the weak charge is universal, and that all the weak reactions which proceed through W exchange can therefore be calculated using the one coupling constant g or G_F . The lifetime of the τ -lepton seemed to illustrate this point: our expectations, based on the assumption that the W boson couples with the same strength to both quarks and leptons were fulfilled. However, the lifetime does not contain the decay widths for leptonic and hadronic processes separately, but only their sum. Furthermore it is very sensitive to the mass of the τ -lepton. Hence, this is not a particularly precise test of weak charge universality.

The coupling to quarks can be better determined from semileptonic hadron decays. This yields a smaller value for the coupling than that obtained from the leptonic muon decay. If a d-quark is transformed into a u-quark, as in the β -decay

²The appearance of further hadronic decay channels will be treated in the next section.

of the neutron, the coupling constant appears to be about 4 % smaller. In processes in which an s-quark is transformed into a u-quark, as in Λ^0 decay, it even appears to be 20 times smaller.

The Cabibbo angle An explanation of these findings was proposed by Cabibbo as early as 1963 [7], at a time at which quarks had not been introduced. We will re-express Cabibbo’s hypothesis in modern terms. We may group the quarks into families, according to their charges and masses, as we did for the leptons:

$$\begin{pmatrix} u \\ d \end{pmatrix} \quad \begin{pmatrix} c \\ s \end{pmatrix} \quad \begin{pmatrix} t \\ b \end{pmatrix}.$$

Quark transitions in the weak decays indeed are observed predominantly within a family but also, to a lesser degree, from one family to another. For charged currents, the “partner” of the flavour eigenstate $|u\rangle$ is therefore not the flavour eigenstate $|d\rangle$, but a linear combination of $|d\rangle$ and $|s\rangle$. We call this linear combination $|d'\rangle$. Similarly the partner of the c-quark is a linear combination of $|s\rangle$ and $|d\rangle$, orthogonal to $|d'\rangle$, which we call $|s'\rangle$.

The coefficients of these linear combinations can be written as the cosine and sine of an angle called the *Cabibbo angle* θ_C . The quark eigenstates $|d'\rangle$ and $|s'\rangle$ of W exchange are related to the eigenstates $|d\rangle$ and $|s\rangle$ of the strong interaction, by a rotation through θ_C :

$$\begin{aligned} |d'\rangle &= \cos \theta_C |d\rangle + \sin \theta_C |s\rangle \\ |s'\rangle &= \cos \theta_C |s\rangle - \sin \theta_C |d\rangle, \end{aligned} \quad (10.18)$$

which may be written as a matrix:

$$\begin{pmatrix} |d'\rangle \\ |s'\rangle \end{pmatrix} = \begin{pmatrix} \cos \theta_C & \sin \theta_C \\ -\sin \theta_C & \cos \theta_C \end{pmatrix} \cdot \begin{pmatrix} |d\rangle \\ |s\rangle \end{pmatrix}. \quad (10.19)$$

Whether the state vectors $|d\rangle$ and $|s\rangle$ or the state vectors $|u\rangle$ and $|c\rangle$ are rotated, or indeed both pairs simultaneously, is a matter of convention alone. Only the difference in the rotation angles is of physical importance. Usually the vectors of the charge $-e/3$ quarks are rotated while those of the charge $+2e/3$ quarks are left untouched. In view of neutrino oscillations that we will discuss in the next chapter we emphasise here that only the eigenstates $|d\rangle$ and $|s\rangle$ of the strong interaction have a well defined mass, but not the states $|d'\rangle$ and $|s'\rangle$.

Experimentally, θ_C is determined by comparing the lifetimes and branching ratios of the semileptonic and hadronic decays of various particles as shown in Fig. 10.10. This yields:

$$\sin \theta_C \approx 0.22, \quad \text{and} \quad \cos \theta_C \approx 0.98. \quad (10.20)$$

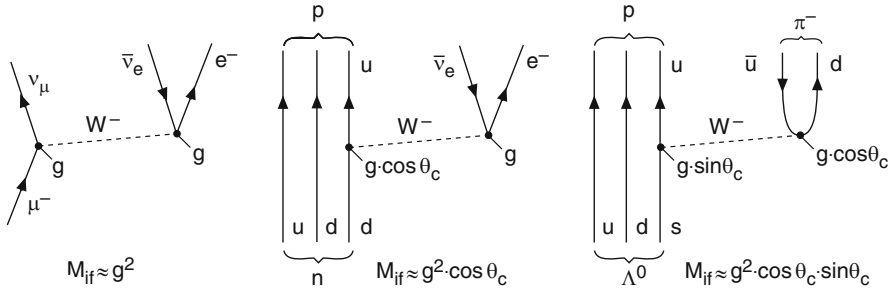


Fig. 10.10 Leptonic decay of the muon (*left*) and the Cabibbo-suppressed semileptonic decays of the neutron (*middle*) and the Λ^0 hyperon (*right*)

The transitions $c \leftrightarrow d$ and $s \leftrightarrow u$, as compared to $c \leftrightarrow s$ and $d \leftrightarrow u$, are therefore suppressed by a factor of

$$\sin^2 \theta_C : \cos^2 \theta_C \approx 1 : 20. \tag{10.21}$$

We can now make our treatment of τ decay more precise. In (10.14), we stated that $\tau \rightarrow \nu_\tau + \bar{u} + d$ is “essentially” the only hadronic decay of the τ . But $\tau \rightarrow \nu_\tau + \bar{u} + s$ is also energetically possible. Whereas the former decay is only slightly suppressed by a factor of $\cos^2 \theta_C$, the latter is faced with a factor of $\sin^2 \theta_C$. However, since $\cos^2 \theta_C$ and $\sin^2 \theta_C$ add to one our conclusion concerning the lifetime of the τ -lepton is not affected, as long as we ignore the difference in the quark masses.

The Cabibbo-Kobayashi-Maskawa matrix Adding the third generation of quarks, the 2×2 matrix of (10.19) is replaced by a 3×3 matrix [15]. This is called the *Cabibbo-Kobayashi-Maskawa matrix* (CKM matrix):

$$\begin{pmatrix} |d'\rangle \\ |s'\rangle \\ |b'\rangle \end{pmatrix} = \begin{pmatrix} V_{ud} & V_{us} & V_{ub} \\ V_{cd} & V_{cs} & V_{cb} \\ V_{td} & V_{ts} & V_{tb} \end{pmatrix} \cdot \begin{pmatrix} |d\rangle \\ |s\rangle \\ |b\rangle \end{pmatrix}. \tag{10.22}$$

The probability for a transition from a quark q_i to a quark q_j is proportional to $|V_{q_i q_j}|^2$, the square of the magnitude of the matrix element.

The matrix elements are correlated since the matrix is unitary. The total number of independent parameters is four: three real angles and an imaginary phase. The phase affects weak processes of higher order via the interference terms. *CP violation* (cf. Sect. 15.5) is attributed to the existence of this imaginary phase [17].

The matrix elements have been determined from a large number of decays and meanwhile are known very well [19]. Their magnitudes are approximately:

$$\left(|V_{ij}| \right) = \begin{pmatrix} 0.974 & 0.225 & 0.003 \\ 0.225 & 0.973 & 0.041 \\ 0.008 & 0.040 & 0.999 \end{pmatrix}. \tag{10.23}$$

The diagonal elements of this matrix describe transitions within a family; they deviate from unity by only a few percent. The values of the matrix elements V_{cb} and V_{ts} are nearly one order of magnitude smaller than those of V_{us} and V_{cd} . Accordingly, transitions from the third to the second generation ($t \rightarrow s$, $b \rightarrow c$) are suppressed by nearly two orders of magnitude compared to transitions from the second to the first generation. This applies to an even higher degree for transitions from the third to the first generation. The direct transition $b \rightarrow u$ was detected in the semileptonic decay of B mesons into non-charmed mesons [2, 3, 13]. Many decays of this kind have been observed during the last decade by the experiments Babar, Belle and CLEO [19].

Weak quark decays only proceed through W exchange. Neutral currents which change the quark flavour (e.g., $c \rightarrow u$) are only possible in higher-order processes and are therefore strongly suppressed in the standard model. The decay $K^+ \rightarrow \pi^+ \nu \bar{\nu}$, for example, has been observed, corresponding to a transition $\bar{s} \rightarrow \bar{d}$. The branching ratio of this decay is $1.5 \cdot 10^{-10}$ [19].

10.5 Parity Violation

A property unique to the weak interaction is parity violation. This means that weak interaction reactions are not invariant under space inversion.

An example of a quantity which changes sign under a spatial inversion is *helicity*

$$h = \frac{\mathbf{s} \cdot \mathbf{p}}{|\mathbf{s}| \cdot |\mathbf{p}|}, \quad (10.24)$$

which we introduced in Sect. 5.3. The numerator is a scalar product of an axial vector (spin) and a vector (momentum). Whereas spin preserves its orientation under mirror reflection, the direction of the momentum is reversed. Thus helicity is a pseudoscalar, changing sign when the parity operator is applied to it. An interaction which depends upon helicity is therefore not invariant under spatial reflections. Helicity is only Lorentz-invariant for massless particles. For particles with a non-vanishing rest mass it is always possible to find a reference frame in which the particle is “overtaken”, i.e., in which its direction of motion and thus its helicity are reversed.

Strictly speaking, helicity has to be distinguished from *chirality*, i.e., handedness. A fermion can be left-handed or right-handed. Helicity and chirality are not to be distinguishable from each other when the fermion mass mc^2 is negligible compared to its energy E . For relativistic fermions, a state with negative helicity is dominantly left-handed, but it also has a small right-handed component. This is suppressed by mc^2/E or $\sqrt{1 - \beta^2}$, where $\beta = v/c$. Right-handed and left-handed states, therefore, have a small admixture of the opposite helicity which is the larger the smaller β .

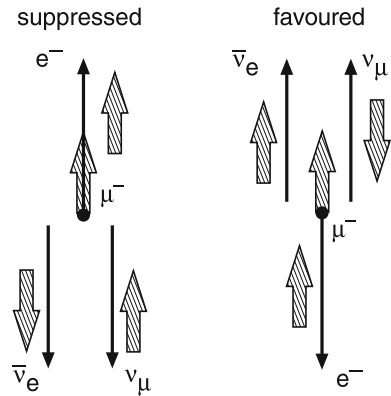
In weak-interaction experiments the participating particles are mostly relativistic and the difference between helicity and chirality is normally irrelevant.

In general, the operator of an interaction described by the exchange of a spin-1 particle can have a vector or an axial vector nature. In order for an interaction to conserve parity, and therefore to couple identically to both right- and left-handed particles, it must be either purely vectorial or purely axial-vectorial. In electromagnetic interactions, for example, it is experimentally observed that only a vector part is present. But in parity-violating interactions, the matrix element has a vector part as well as an axial vector part. Their strengths are described by two coefficients, c_V and c_A . The closer the size of the two parts the stronger is the parity violation. *Maximum parity violation* occurs if both contributions are equal in magnitude. A $(V+A)$ interaction, i.e., a sum of vector and axial interactions of equal strength ($c_V = c_A$), couples exclusively to right-handed fermions and left-handed antifermions. A $(V-A)$ interaction ($c_V = -c_A$) only couples to left-handed fermions and right-handed antifermions.

As we will show, the angular distribution of electrons produced in the decay of polarised muons exhibits parity violation. This decay can be used to measure the ratio c_V/c_A . Such experiments yield $c_V = -c_A = 1$ for the coupling strength of W bosons to leptons. One therefore speaks of a *V-minus-A theory* of charged currents. Parity violation is maximal. If a neutrino or an antineutrino is produced by W exchange, the neutrino helicity is negative, while the antineutrino helicity is positive. Indeed all experiments are consistent with *neutrinos being always left-handed and antineutrinos right-handed*. We will describe such an experiment in Sect. 18.6.

Parity violation in muon decay An instructive example of parity violation is the muon decay $\mu^- \rightarrow e^- + \nu_\mu + \bar{\nu}_e$. In the rest frame of the muon, the momentum of the electron is maximised if the momenta of the neutrinos are parallel to each other, and antiparallel to the momentum of the electron. From Fig. 10.11 it is apparent that the spin of the emitted electron must be in the same direction as that of the muon since the spins of the $(\nu_e, \bar{\nu}_\mu)$ pair cancel.

Fig. 10.11 Parity-violating decay of a polarised muon, $\mu^- \rightarrow e^- + \nu_\mu + \bar{\nu}_e$. Electrons are emitted preferentially with their spin opposite to their momentum (*right*)



Experimentally it is observed that electrons from polarised muon decays are preferentially emitted with their spin opposite to their momentum; i.e., they are left-handed. This left-right asymmetry is a manifestation of parity violation. The ratio of the vector to axial vector strengths can be determined from the angular distribution [6].

Helicity suppressed pion decay Our second example is the decay of the charged pion. The lightest hadron with electric charge, the π^- , can only decay in a semileptonic weak process, i.e., through a charged current, according to

$$\begin{aligned}\pi^- &\rightarrow \mu^- + \bar{\nu}_\mu, \\ \pi^- &\rightarrow e^- + \bar{\nu}_e.\end{aligned}$$

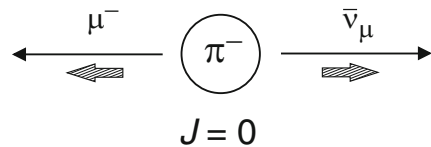
The muon mass is only slightly smaller than the pion mass, therefore in pion decay the muon is non-relativistic and we have to distinguish between helicity and chirality. The second process is suppressed, compared to the first one, by a factor of 1:8,000 [5] (cf. Table 15.3). From the amount of phase space available, however, one would expect the pion to decay about 3.5 times more often into an electron than into a muon. This behaviour may be explained from helicity considerations.

The particles created in such two-particle pion decays are emitted, in the centre-of-mass system, in opposite directions. Since the pion has spin zero, the spins of the two leptons must be opposite to each other. Thus, the projections on the direction of motion are either $+1/2$ for both, or $-1/2$ for both. The latter case is impossible as the helicity of antineutrinos is fixed. Therefore, the spin projection of the muon (electron) is $+1/2$ (Fig. 10.12).

If electrons and muons were massless, two-body pion decays would be forbidden. A massless electron, or muon, would have to be 100% right-handed, but W bosons only couple to left-handed leptons. Because of their finite mass, electrons and muons with their spins pointing in their directions of motion actually also have a left-handed component. This leads to a factor $(1 - \beta)$ in the decay width (Fig. 10.12). The W boson couples to this component. Since the electron mass is so small, $1 - \beta_e = 2.6 \cdot 10^{-5}$ is very small in pion decay, compared to $1 - \beta_\mu = 0.72$. Hence, the left-handed component of the electron is far smaller than that of the muon, and the electron decay is accordingly strongly suppressed.

CP conservation It may be easily seen that if the helicity of the neutrinos is fixed, then *C-parity* (“charge conjugation”) is simultaneously violated. Application of the C-parity operator replaces all particles by their antiparticles. Thus, left-handed

Fig. 10.12 Allowed spin projections of μ^- and $\bar{\nu}_\mu$ in π^- decay



neutrinos would be transformed into left-handed antineutrinos, which do not appear in the standard model. Therefore, physical processes which involve neutrinos, and in general all weak processes, a priori violate C-parity. The combined application of space inversion (P) and of charge conjugation (C), however, yields a process which is physically possible. Here, left-handed fermions are transformed into right-handed antifermions, which interact with equal strength. This is called the *CP conservation* property of the weak interaction. Cases in which CP symmetry is not conserved (CP violation) will be discussed in Sects. 15.4 and 15.5.

10.6 Deep-Inelastic Scattering with Charged Currents

Deep-inelastic scattering of neutrinos Deep-inelastic scattering of neutrinos and antineutrinos off nucleons gives us information about the quark distributions in the nucleon which cannot be obtained from electron or muon scattering alone. In contrast to photon exchange, the exchange of W bosons (charged currents) in neutrino scattering distinguishes between the helicity and charged states of the fermions involved. This is then exploited to separately determine the quark and antiquark distributions in the nucleon.

In deep-inelastic neutrino scattering experiments, muon (anti)neutrinos are generally used, which, as discussed in Sect. 10.5, stem from weak pion and kaon decays. These latter particles can be produced in large numbers by bombarding a solid block of material with a beam of high-energy protons. After a several hundred metre long decay line the decay muons are ranged out by a long shield of iron and soil. What remains is a beam of neutrinos impinging on a target. Since (anti)neutrinos have very small cross-sections the targets that are used (e.g., iron) are generally many metres long. The deep-inelastic scattering takes place off both the protons and the neutrons in the target.

When left-handed neutrinos scatter off nucleons, the exchanged W^+ can only interact with the negatively charged, left-handed quarks (d_L, s_L) and negatively charged, right-handed antiquarks (\bar{u}_R, \bar{c}_R) which are thereby transformed into the corresponding (anti)quarks of the same family (Fig. 10.13 (left)). In analogy to

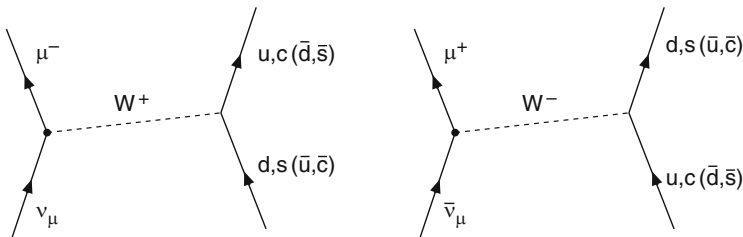


Fig. 10.13 Charged-current interactions of neutrinos (*left*) and antineutrinos (*right*) with the possible selected quark and antiquark flavours

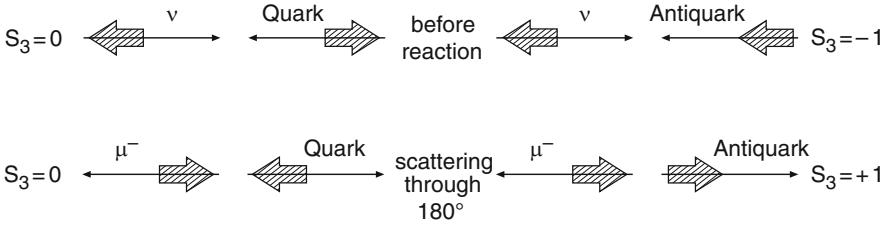


Fig. 10.14 Charged-current νq scattering (left) and $\nu \bar{q}$ scattering (right) before the reaction (top) and after scattering through 180° in the neutrino-quark centre-of-mass system

our description of τ decay, we can neglect complications due to Cabibbo mixing if the energies are large enough that we can ignore the differences in the quark masses. Equivalently for the scattering of right-handed antineutrinos, the W^- which is exchanged can only interact with the positively charged, left-handed quarks (u_L, c_L) and positively charged, right-handed antiquarks (\bar{d}_R, \bar{s}_R) (Fig. 10.13 (right)).

Separation of quark and antiquark distributions The scattering off the quarks and antiquarks is characterised by different angle and energy distributions for the outgoing leptons. This becomes plausible if one (analogously to our considerations in the case of Mott scattering in Sect. 5.3) considers the extreme case of scattering through $\theta_{c.m.} = 180^\circ$ in the centre-of-mass frame for the neutrino and the quark (Fig. 10.14). We choose the quantisation axis \hat{z} to be the momentum direction of the incoming neutrino. Since the W boson only couples to left-handed fermions, both the neutrino and the quark have in the high-energy limit negative helicities and the projection of the total spin on the \hat{z} axis is, both before and after scattering through 180° $S_3 = 0$.

This also holds for all other scattering angles, i.e., the scattering is isotropic.

On the other hand if a left-handed neutrino interacts with a right-handed antiquark, the spin projection before the scattering is $S_3 = -1$ but after being scattered through 180° it is $S_3 = +1$. Hence scattering through 180° is forbidden by conservation of angular momentum. An angular dependence, proportional to $(1 + \cos \theta_{c.m.})^2$, is found in the differential cross-section. In the laboratory frame this corresponds to an energy dependence proportional to $(1 - y)^2$ where

$$y = \frac{E_{\nu, \bar{\nu}} - E'_\mu}{E_{\nu, \bar{\nu}}} \tag{10.25}$$

is that fraction of the neutrino energy which is transferred to the quark. Completely analogous considerations hold for antineutrino scattering.

The cross-section for neutrino-nucleon scattering may be written analogously to the cross-section for neutrino-electron scattering (10.9) if we take into account the fact that the interacting quark only carries a fraction x of the momentum of the

nucleon and that the centre-of-mass energy in the neutrino-quark centre-of-mass system is x times smaller than in the neutrino-nucleon system. For an isoscalar target the double differential cross-section per (proton-neutron average) nucleon then reads:

$$\frac{d^2\sigma^{\nu,\bar{\nu}-N}}{dx dy} = \sigma_0^{\nu,\bar{\nu}-N} \cdot K^{\nu,\bar{\nu}-N}(x, y), \quad (10.26)$$

where

$$\sigma_0^{\nu,\bar{\nu}-N} = \frac{G_F^2}{\pi(\hbar c)^4} \cdot \left(\frac{M_W^2 c^4}{Q^2 c^2 + M_W^2 c^4} \right)^2 \cdot M_p c^2 E^{\nu,\bar{\nu}} \quad (10.27)$$

and

$$K^{\nu-N}(x, y) = x[u(x) + d(x) + 2s_s(x) + (\bar{u}_s(x) + \bar{d}_s(x) + 2\bar{c}_s(x))(1-y)^2], \quad (10.28)$$

$$K^{\bar{\nu}-N}(x, y) = x[\bar{u}_s(x) + \bar{d}_s(x) + 2\bar{s}_s(x) + (u(x) + d(x) + 2c_s(x))(1-y)^2]. \quad (10.29)$$

The latter equations hold in the quark-parton model assuming isospin symmetry for the quark distributions and with $u(x) = u_v(x) + u_s(x)$ and $d(x) = d_v(x) + d_s(x)$.

Figure 10.15 shows the dependence of the differential cross-section $d\sigma/dy$ as a function of y upon integration over x . For neutrino scattering we have two contributions: a large constant contribution from scattering off the quarks, and a small contribution from scattering off the antiquarks which falls off as $(1-y)^2$. In antineutrino scattering one observes a strong $(1-y)^2$ dependence from the

Fig. 10.15 Differential cross-sections $d\sigma/dy$ for neutrino and antineutrino scattering off nucleons as a function of y (in arbitrary units)

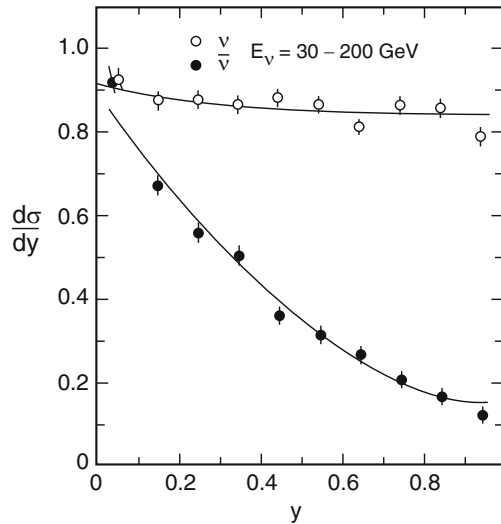
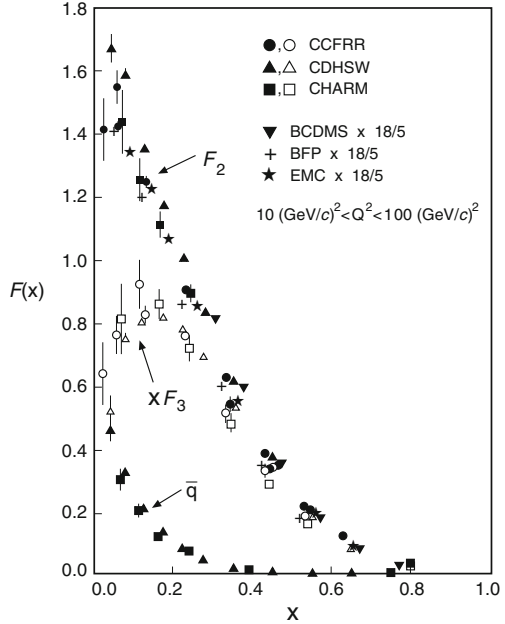


Fig. 10.16 Comparison of the structure function $F_2(x)$ per proton-neutron averaged nucleon, measured in deep-inelastic scattering of muons and neutrinos [18]. Also shown is the structure function $x F_3(x)$ which describes the distribution of valence quarks, and the distribution of antiquarks $\bar{q}(x)$ which yields the sea quark distribution



interaction with the quarks and a small energy independent part from the antiquarks. Suitable combinations of the data from neutrino and antineutrino scattering off protons and neutrons can be used to separate the distributions of valence and sea quarks shown in Fig. 10.16.

Structure functions in deep-inelastic neutrino scattering In Chap. 7 we have expressed the cross-section for deep-inelastic scattering of charged leptons off nucleons (7.10) in terms of the *two* structure functions $F_1(x, Q^2)$ and $F_2(x, Q^2)$. Similarly also the cross-section for deep-inelastic neutrino-nucleon scattering can be written in terms of *three* structure functions $F_i(x, Q^2)$ ($i = 1, 2, 3$), three each for νp , $\bar{\nu} p$, νn , and $\bar{\nu} n$ scattering:

$$\frac{d^2\sigma^{\nu,\bar{\nu}}}{dx dy} = \sigma_0^{\nu,\bar{\nu}} \cdot \left[\left(1 - y - xy \frac{Mc^2}{2E^{\nu,\bar{\nu}}} \right) F_2^{\nu,\bar{\nu}} + \frac{y^2}{2} 2xF_1^{\nu,\bar{\nu}} \pm y \left(1 - \frac{y}{2} \right) xF_3^{\nu,\bar{\nu}} \right]. \quad (10.30)$$

Here the x and Q^2 dependence of the structure functions has been omitted for brevity. The structure function $x F_3^{\nu,\bar{\nu}}$ appears here for the first time. It is a consequence of the parity violating ($V-A$) structure of the weak charged current. The term with $x F_3^{\nu,\bar{\nu}}$ has positive sign for neutrino scattering and negative sign for antineutrino scattering. Equation (10.30) is also valid in the kinematic region of small values of Q^2 , where the quark-parton model can no longer be used for the

interpretation of the data. Assuming $2xF_1^{v,\bar{v}} = F_2^{v,\bar{v}}$, we obtain in the region of sufficiently high values of Q^2 from Eqs. (10.26) to (10.30) the following relations between the structure functions for the proton-neutron averaged nucleon and the quark distributions:

$$xF_3^N(x) = \frac{1}{2}[xF_3^{v-N}(x) + xF_3^{\bar{v}-N}(x)] = x[u_v(x) + d_v(x)], \quad (10.31)$$

$$F_2^{v-N}(x) = F_2^{\bar{v}-N}(x) = x \sum_{q=d,u,s,c} [q(x) + \bar{q}_s(x)], \quad (10.32)$$

$$\bar{q}^{\bar{v}-N}(x) = x [\bar{u}_s(x) + \bar{d}_s(x) + 2\bar{s}_s(x)], \quad (10.33)$$

with $q(x) = q_v(x) + q_s(x)$ for u- and d-quarks and $q(x) = q_s(x)$ for s- and c-quarks.

Thus, comparing (10.32) and (7.24) we see that apart from small corrections for the contributions of the heavier s- and c-quarks the structure functions F_2 per proton-neutron averaged nucleon in electron and neutrino scattering are related by

$$F_2^{v-N}(x) \simeq \frac{18}{5} F_2^{e-N}(x). \quad (10.34)$$

In Fig. 10.16 data from deep-inelastic scattering experiments of the second generation with muon beams (BCDMS, BFP, EMC) and neutrino beams (CCFR, CDHSW, CHARM) are presented as a function of x in the Q^2 range 10–100 (GeV/c)².

The structure functions $F_2(x)$ per proton-neutron averaged nucleon are essentially equal, apart from the factor 18/5. This is again a confirmation for the proper assignment of the fractional quark charges $+2e/3$ for u- and c-quarks and $-1e/3$ for d- and s-quarks. We also see from this figure that the sea-quark distribution $\bar{q}(x)$ falls off steeply with x and is negligible for $x > 0.35 - 0.4$. At larger values of x only valence quarks contribute to F_2 ; their distribution has a maximum near $x \approx 0.17$.

Polarised deep-inelastic scattering at high Q^2 The two experiments H1 and ZEUS at HERA mainly investigated deep-inelastic events of the type $e^\pm + p \rightarrow e'^\pm + X$, where the interaction between lepton and nucleon is mediated by the exchange of a virtual photon or a Z^0 boson. Occasionally also events of the type $e^\pm + p \rightarrow X$ occurred where no scattered electron or positron was observed in the detector. These were attributed to the reactions $e^- + p \rightarrow \nu_e + X$ or $e^+ + p \rightarrow \bar{\nu}_e + X$, respectively (Fig. 10.17).

In these reactions the interaction is mediated by the exchange of W^\pm bosons, i.e., by charged currents. Due to the hermetic 4π -detectors, the kinematics of these events could be fully reconstructed from the tracks and energies of the quark fragments and the remnants of the struck proton (cf. Fig. 8.6).

The lepton beam in the HERA storage ring could be longitudinally polarised. This happened as follows: based on an asymmetry in the spin-flip probability

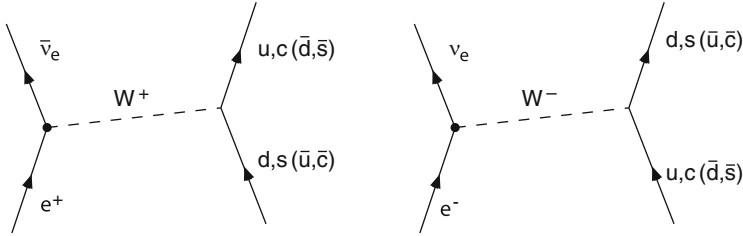


Fig. 10.17 Charged-current reactions in deep-inelastic positron (*left*) and electron (*right*) scattering off nucleons

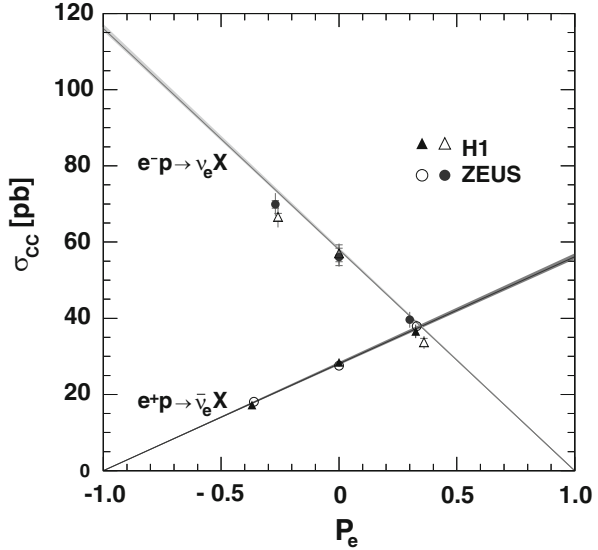
for the emission of synchrotron radiation, the spins of the circulating electrons gradually became oriented antiparallel to the direction of the magnetic fields in the arcs (Sokolov-Ternov-Effect [20], cf. Problem 10.6). A system of magnets, so-called spin rotators, on both sides of the experiments changed this transverse polarisation of the beam into a longitudinal one and back again to transverse behind the experiments. The degree of longitudinal polarisation P_e is given by $P_e = (N^{\rightarrow} - N^{\leftarrow}) / (N^{\rightarrow} + N^{\leftarrow})$. Here N^{\rightarrow} (N^{\leftarrow}) is the number of electrons with spin orientation parallel (antiparallel) to the beam momentum. Neutrinos are always left-handed. But here we can choose the handedness: electrons or positrons with positive polarisation are predominantly right-handed, those with negative polarisation are predominantly left-handed.

The cross-section for charged-current reactions depends linearly on the lepton-beam polarisation:

$$\sigma_{CC}^{e^{\pm}p}(P_e) = (1 \pm P_e) \sigma_{CC}^{e^{\pm}p}(P_e = 0), \quad (10.35)$$

where the minus sign holds for electrons. For $P_e = +1$ the cross-section for the reaction $e^- + p \rightarrow \nu_e + X$ should vanish, since by helicity conservation a right-handed electron cannot be transformed into a left-handed neutrino, while the cross-section is maximal for $P_e = -1$. For positrons the situation is just reversed. The experimental data of H1 and ZEUS excellently confirm these considerations. In Fig. 10.18 the charged-current cross-sections σ_{CC} for electrons and positrons are shown as a function of the degree of longitudinal polarisation P_e [1]. The data fulfil the requirements $Q^2 > 400$ (GeV/c) 2 and $y > 0.9$. As expected, they lie on a straight line. The extrapolation to either $P_e = +1$ or $P_e = -1$ provides information about the possible existence of right-handed charged currents which are excluded in the standard model of particle physics (cf. Chap. 13). No deviations from this expectation are observed. In addition, the data show another interesting feature: the maximal cross-sections for electrons and positrons are of different magnitude. This observation can be easily traced back to the circumstance that the W^- boson

Fig. 10.18 The cross-section σ_{CC} of deep-inelastic scattering of electrons and positrons with charged currents as a function of the beam polarisation P_e



exchanged in electron scattering couples preferentially to the u-quark, while in positron scattering the exchanged W^+ boson couples preferentially to the d-quark, and that the quark distribution $u(x)$ is nearly a factor of two larger than the quark distribution $d(x)$.

Problems

1. Particle reactions

Show whether the following particle reactions and decays are possible or not. State which interaction is concerned and sketch the quark composition of the hadrons involved.

$$\begin{aligned}
 p + \bar{p} &\rightarrow \pi^+ + \pi^- + \pi^0 + \pi^+ + \pi^- \\
 p + K^- &\rightarrow \Sigma^+ + \pi^- + \pi^+ + \pi^- + \pi^0 \\
 p + \pi^- &\rightarrow \Lambda^0 + \bar{\Sigma}^0 \\
 \bar{\nu}_\mu + p &\rightarrow \mu^+ + n \\
 \nu_e + p &\rightarrow e^+ + \Lambda^0 + K^0 \\
 \Sigma^0 &\rightarrow \Lambda^0 + \gamma
 \end{aligned}$$

2. Parity and C-parity

(a) Which of the following particle states are eigenstates of the charge conjugation operator \mathcal{C} and what are their respective eigenvalues?

$$|\gamma\rangle; |\pi^0\rangle; |\pi^+\rangle; |\pi^-\rangle; |\pi^+\rangle - |\pi^-\rangle; |\nu_e\rangle; |\Sigma^0\rangle.$$

- (b) How do the following quantities behave under the parity operation? (Supply a brief explanation.)

Position vector \mathbf{r}	Momentum \mathbf{p}
Angular momentum \mathbf{L}	Spin $\boldsymbol{\sigma}$
Electric field \mathbf{E}	Magnetic field \mathbf{B}
Electric dipole moment $\boldsymbol{\sigma} \cdot \mathbf{E}$	Magnetic dipole moment $\boldsymbol{\sigma} \cdot \mathbf{B}$
Helicity $\boldsymbol{\sigma} \cdot \mathbf{p}$	Transversal polarisation $\boldsymbol{\sigma} \cdot (\mathbf{p}_1 \times \mathbf{p}_2)$

3. **Parity and C-parity of the f_2 -mesons** The $f_2(1270)$ -meson has spin 2 and decays, amongst other routes, into $\pi^+\pi^-$.

- (a) Use this decay to find the parity and C-parity of the f_2 .
 (b) Investigate whether the decays $f_2 \rightarrow \pi^0\pi^0$ and $f_2 \rightarrow \gamma\gamma$ are allowed.

4. Pion decay and the Golden Rule

Calculate the ratio of the partial decay widths

$$\frac{\Gamma(\pi^+ \rightarrow e^+\nu)}{\Gamma(\pi^+ \rightarrow \mu^+\nu)}$$

and so verify the relevant claims in the text. From the Golden Rule it holds that $\Gamma(\pi \rightarrow \ell\nu) \propto |\mathcal{M}_{\pi\ell}|^2 \varrho(E_0)$, where $|\mathcal{M}_{\pi\ell}|$ is the transition matrix element and $\varrho(E_0) = dn/dE_0$ is the density of states (ℓ denotes the charged lepton). The calculation may be approached as follows:

- (a) Derive formulae for the momenta and energies of the charged leptons ℓ^+ as functions of m_ℓ and m_π and so find numerical values for $1 - v/c$.
 (b) We have $|\mathcal{M}_{\pi\ell}|^2 \propto 1 - v/c$. Use this to express the ratio of the squares of the matrix elements as a function of the particle masses involved and find its numerical value.
 (c) Calculate the ratio of the densities of states $\varrho_e(E_0)/\varrho_\mu(E_0)$ as a function of the masses of the particles involved. Exploit the fact that the density of states in momentum space is $dn/d|\mathbf{p}| \propto |\mathbf{p}|^2$ ($|\mathbf{p}| = |\mathbf{p}_{\ell^+}| = |\mathbf{p}_\nu|$) and that $E_0 = E_{\ell^+} + E_\nu$. For which of the two decays is the “phase space” bigger?
 (d) Combine the results from (b) and (c) to obtain the ratio of the partial decay widths as a function of the masses of the particles involved. Find its numerical value and compare it with its experimental value of $(1.230 \pm 0.004) \cdot 10^{-4}$.

5. Spin polarisation of muon beams

Muons are used to carry out deep inelastic scattering experiments at high beam energies. First a static target is bombarded with a proton beam. This produces charged pions which decay in flight into muons and neutrinos.

- (a) What is the energy range of the muons in the laboratory frame if magnetic fields are used to select a 350 GeV pion beam?
- (b) Why are the spins of such a monoenergetic muon beam polarised? How does the polarisation vary as a function of the muon energy?

6. Compton scattering

At the HERA collider ring the spins of the electrons going around the ring align themselves over time antiparallel to the magnetic guide fields (Sokolov-Ternov effect [20]). This spin polarisation may be measured with the help of the spin dependence of Compton scattering. We solely consider the kinematics below.

- (a) Circularly polarised photons from an argon laser (514 nm) hit the electrons (26.67 GeV, straight flight path) head on. What energy does the incoming photon have in the rest frame of the electron?
- (b) Consider photon scattering through 90° and 180° in the electron rest frame. What energy does the scattered photon possess in each case? How large are the energies and scattering angles in the lab frame?
- (c) How good does the spatial resolution of a calorimeter have to be if it is 64 m away from the interaction vertex and should spatially distinguish between these photons?

References

1. F.D. Aaron et al., JHEP **1209**, 061 (2012)
2. H. Albrecht et al., Phys. Lett. **B234**, 409 (1990)
3. H. Albrecht et al., Phys. Lett. **B255**, 297 (1991)
4. B.C. Barish, R. Stroynowski, Phys. Rep. **157**, 1 (1988)
5. D.I. Britton et al., Phys. Rev. Lett. **68**, 3000 (1992)
6. H. Burkard et al., Phys. Lett. **B160**, 343 (1985)
7. N. Cabibbo, Phys. Rev. Lett. **10**, 531 (1963)
8. J.H. Christenson, J.W. Cronin, V.L. Fitch, R. Turlay, Phys. Rev. Lett. **13**, 138 (1964)
9. E.D. Commins, *Weak Interactions* (McGraw-Hill, New York, 1973)
10. C.L. Cowan Jr., F. Reines et al., Science **124**, 103 (1956)
11. G. Danby et al., Phys. Rev. Lett. **9**, 36 (1962)
12. E. Fermi, Z. Phys. **88**, 161 (1934)
13. R. Fulton et al., Phys. Rev. Lett. **64**, 16 (1990)
14. F.J. Hasert et al., Phys. Lett. **B46**, 138 (1973)
15. M. Kobayashi, T. Maskawa, Prog. Theor. Phys. **49**, 652 (1973)
16. W.J. Marciano, Annu. Rev. Nucl. Part. Sci. **41**, 469 (1991)
17. E.A. Paschos, U. Türke, Phys. Rep. **178**, 145 (1989)
18. Particle Data Group, L. Montanet et al., *Review of Particle Properties*. Phys. Rev. **D50**, 1173 (1994)
19. Particle Data Group, J. Beringer et al., *Review of Particle Properties*. Phys. Rev. D **86**, 010001 (2012)
20. A.A. Sokolov, J.M. Ternov, Sov. Phys. Dokl. **8**, 1203 (1964)
21. C.S. Wu et al., Phys. Rev. **105**, 1413 (1957)